0026-895X/09/7503-454–465$20.00
MOLECULAR PHARMACOLOGY
Copyright © 2009 The American Society for Pharmacology and Experimental Therapeutics
Mol Pharmacol 75:454–465, 2009

Vol. 75, No. 3
53009/3436657
Printed in U.S.A.

Molecular Basis for the Selective Interaction of Synthetic Agonists with the Human Histamine H_1-Receptor Compared with the Guinea Pig H_1-Receptor

Andrea Straßer, Hans-Joachim Wittmann, Marc Kunze,[1] Sigurd Elz, and Roland Seifert

Department of Pharmaceutical/Medicinal Chemistry I, School of Pharmacy (A.S., M.K., S. E.) and Faculty of Chemistry and Pharmacy (H.-J.W.), University of Regensburg, Regensburg, Germany; and Institute of Pharmacology, Medical School of Hannover, Hannover, Germany (R.S.)

Received October 23, 2008; accepted December 1, 2008

ABSTRACT

Previous studies revealed that phenylhistamines and histaprodifens possess higher potency and affinity at guinea pig histamine H_1-receptor (gpH_1R) than at human histamine H_1-receptor (hH_1R). However, we recently identified an imidazolylpropylguanidine [N^1-(3-cyclohexylbutanoyl)-N^2-[3-(1*H*-imidazol-4-yl)-propyl]guanidine (UR-AK57)] with higher potency and efficacy at hH_1R compared with gpH_1R. The aim of this study was to reveal the molecular basis for the species differences of synthetic ligands. We studied 11 novel phenylhistamines and phenoprodifens. H_1R species isoforms were expressed in Sf9 insect cells, and [^{3}H]mepyramine competition binding and GTPase assays were performed. We identified bulky phenylhistamines with higher potency and affinity at hH_1R compared with gpH_1R. Molecular dynamics simulations of ligand-H_1R interactions revealed four potential binding modes for phenylhistamines possessing an additional histamine moiety; the terminal histamine moiety showed a high flexibility in the binding pocket. There are striking similarities in ligand properties in bulky phenylhistamines and UR-AK57. Comparison of bulky phenylhistamine binding mode with binding mode of UR-AK57 suggests that only one of these four binding modes should be established. The higher potency is explained by more effective van der Waals interaction of the compounds with $Asn^{2.61}$ (hH_1R) relative to $Ser^{2.61}$ (gpH_1R). In addition, two stable binding modes for phenoprodifens with different orientations in the binding-pocket were identified. Depending on phenoprodifen orientation, the highly conserved $Trp^{6.48}$, part of the toggle switch involved in receptor activation, was found in an inactive or active conformation, respectively. We identified the first phenylhistamines with higher potency at hH_1R than at gpH_1R and obtained insight into the binding mode of bulky phenylhistamines and imidazolylpropylguanidines.

The biogenic amine histamine binds to, and activates, histamine receptors. Histamine mediates a variety of physiological and pathophysiological effects. All histamine receptors belong to the rhodopsin-like G-protein-coupled receptors (GPCRs). Meanwhile, four histamine receptor subtypes have been cloned: the histamine H_1 receptor (H_1R) (Moguilevsky et al., 1994), the histamine H_2 receptor (H_2R) (Gantz et al., 1991), the histamine H_3 receptor (H_3R) (Lovenberg et al., 1999) and the histamine H_4 receptor (H_4R) (Oda et al., 2000). The H_1R interacts with G_q-proteins to activate phospholipase C (Hill et al., 1997). H_1R antagonists, divided into first- and second-generation antagonists, are used therapeutically, whereas H_1R agonists are important tools to study the pharmacology of the H_1R at the molecular level. Different classes of H_1R agonists are known, including small agonists derived from histamine (**1** in Fig. 1) and bulkier agonists such as phenylhistamines (**2**, **4**, and **6** in Fig. 1) (Leschke et al., 1995; Zingel et al., 1995), ergolines (Pertz et al., 2006), and histaprodifens (**12** and **17** in Fig. 1) (Elz et al., 2000; Menghin et al., 2003). In addition, imidazolypropylguanidines, originally designed as selective H_2R agonists, act as partial H_1R agonists, too (Xie et al., 2006). In fact, the imidazolylpropylguanidine UR-AK57 (**19** in Fig. 1) (Xie et al., 2006) is the first synthetic agonist that shows higher potency at hH_1R than at gpH_1R.

$Asn^{2.61}$ acts as a selectivity switch between hH_1R and gpH_1R (Bruysters et al., 2005) for suprahistaprodifen (Menghin et al., 2003). Our recent study with histaprodifens at

This work was supported by the Deutsche Forschungsgemeinschaft [Grant GRK760] and by the Research Training Program (Graduiertenkolleg) "Medicinal Chemistry: Molecular Recognition-Ligand-Receptor Interactions."

[1] Current affiliation: Abbott GmbH and Co. KG, Wiesbaden, Germany.

Article, publication date, and citation information can be found at http://molpharm.aspetjournals.org.
doi:10.1124/mol.108.053009.

ABBREVIATIONS: GPCR, G-protein-coupled receptor; H_nR, histamine H_n receptor (where *n* is 1–4); UR-AK57, N^1-(3-cyclohexylbutanoyl)-N^2-[3-(1*H*-imidazol-4-yl)propyl]guanidine; h, human; gp, guinea pig; b, bovine; r, rat; MD, molecular dynamics; TM, transmembrane domain; hH_2R-$G_s\alpha_S$, fusion protein of the human histamine H_2R and the short splice variant of $G_s\alpha$.

hH_1R and gpH_1R corroborated the fact that $Asn^{2.61}$ acts as selectivity switch (Straßer et al., 2008b).

Several phenylhistamines and histaprodifens (Seifert et al., 2003), as well as ergolines (Pertz et al., 2006), were studied at the recombinant guinea pig H_1-receptor (gpH_1R) and human H_1-receptor (hH_1R) expressed in Sf9 insect cell membranes by [^{3}H]mepyramine competition binding and G_q-protein-catalyzed GTP hydrolysis. In general, the affinity of phenylhistamines and histaprodifens is higher at gpH_1R than at hH_1R (Seifert et al., 2003). Because a more recent study revealed species differences for histaprodifens between hH_1R, bovine H_1-receptor (bH_1R), rat H_1-receptor (rH_1R), and gpH_1R (Straßer et al., 2008a), we also expect species differences in pharmacology for members of several subclasses of phenylhistamines: 1) small phenylhistamines (Fig. 1, **2**-**6**), 2) bulky phenylhistamines with an additional histamine moiety (Fig. 1, **7**-**9**), 3) dimeric phenylhistamines (Fig. 1, **10** and **11**), and 4) phenoprodifens (phenylhistamines coupled to a histaprodifen partial structure) (Fig. 1, **13**-**16**). To study the H_1R-species-dependent pharmacology of these compounds, we coexpressed hH_1R, bH_1R, rH_1R, or gpH_1R with the regulator of G-protein signaling RGS4 in Sf9 insect cells and characterized known and 11 novel phenylhistamines and phenoprodifens (Fig. 1) in [^{3}H]mepyramine competition binding and GTPase assays. The pharmacological analysis of synthetic ligands, not only at hH_1R, but also at bH_1R, rH_1R and gpH_1R, is a standard technique, taking advantage of the differences in amino acid sequence between H_1R species isoforms as natural mutations (Straßer et al., 2008a). This technique allows us to obtain useful information about the interactions of amino acids with the ligand in the binding pocket. Beyond the H_1R, the analysis of receptor species isoforms has also been most valuable for the H_2R (Preuss et al., 2007a), H_3R (Ligneau et al., 2000), and H_4R (Thurmond et al., 2004).

To obtain information about the binding mode of bulky phenylhistamines and phenoprodifens, we docked these compounds into active state models of gpH_1R and hH_1R (Straßer

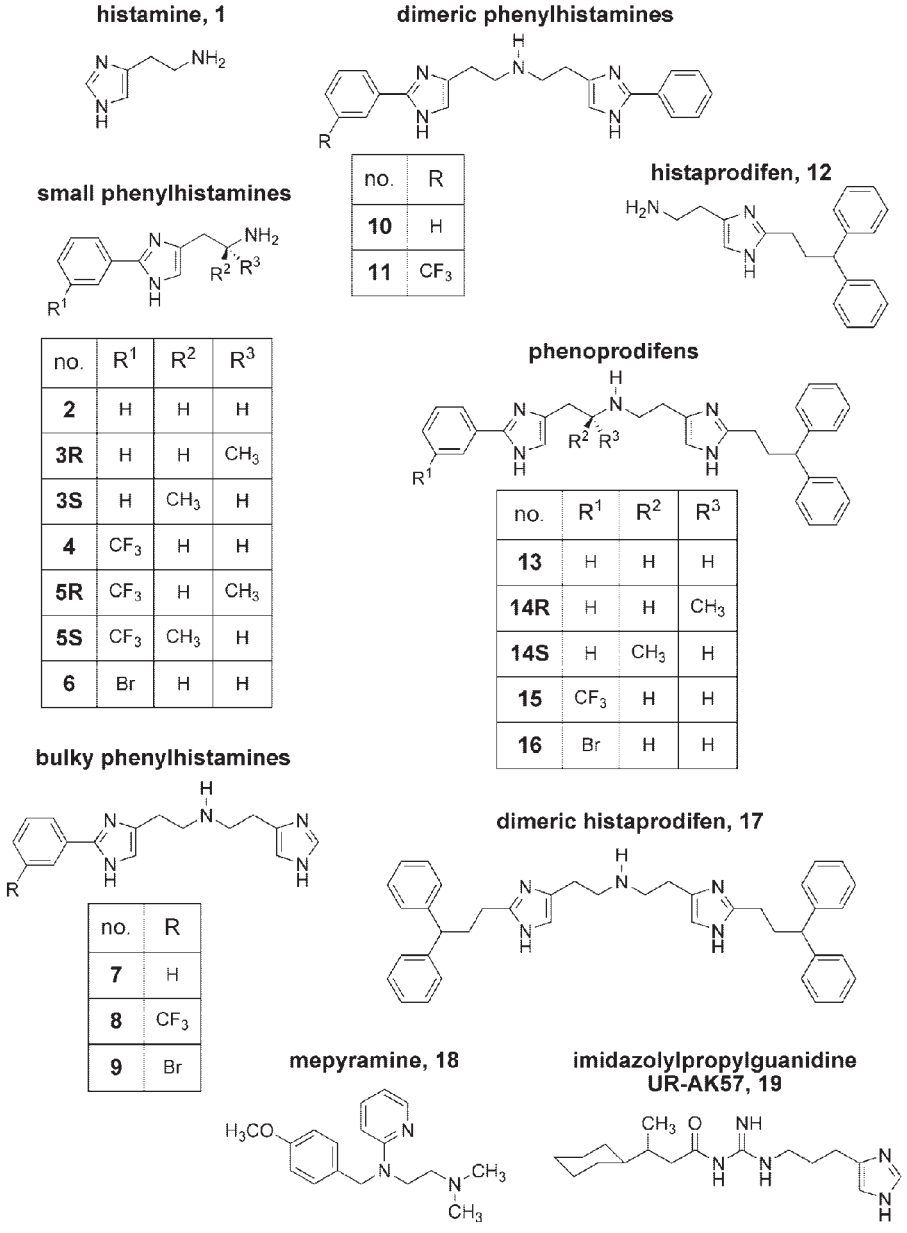

no.	R
10	H
11	CF_3

no.	R^1	R^2	R^3
2	H	H	H
3R	H	H	CH_3
3S	H	CH_3	H
4	CF_3	H	H
5R	CF_3	H	CH_3
5S	CF_3	CH_3	H
6	Br	H	H

no.	R^1	R^2	R^3
13	H	H	H
14R	H	H	CH_3
14S	H	CH_3	H
15	CF_3	H	H
16	Br	H	H

no.	R
7	H
8	CF_3
9	Br

Fig. 1. Structures of histamine, phenylhistamines, phenoprodifens, mepyramine, and imidazolylpropylguanidine UR-AK57. Histamine **1**, small phenylhistamines **2**-**6**, bulky phenylhistamines with an additional histamine moiety **7** to **9**, dimeric phenylhistamines **10** and **11**, histaprodifen **12**, phenoprodifens **13** to **16**, dimeric histaprodifen **17**, mepyramine **18**, and imidazolylpropylguanidine **19** (UR-AK57).

et al., 2008a,b) and performed molecular dynamics (MD) simulations, including the surrounding of the receptor.

Materials and Methods

Materials. [γ-^{32}P]GTP was synthesized as described previously (Preuss et al., 2007b). [^{3}H]Mepyramine (30.0 Ci/mmol) was from PerkinElmer Life and Analytical Sciences (Walatham, MA). Rotiszint Eco Plus from Roth (Karlsruhe, Germany) was used as liquid scintillation cocktail. Phenylhistamines and phenoprodifens were synthesized as described previously (Kunze, 2006). Sources of all other materials were described previously (Seifert et al., 2003; Straßer et al., 2008a,b).

Preparation of Compound Stock Solutions. Chemical structures of the analyzed compounds are given in Fig. 1. Compounds **2** to **9** (10 mM each) were dissolved in double-distilled water. Compounds **10**, **11**, **15**, and **16** (5 mM each) were dissolved in a solvent containing 50% (v/v) DMSO and 50% (v/v) double-distilled water. All other ligands were dissolved as described previously (Straßer et al., 2008a). The final DMSO concentration in all assays was adjusted to 5% (v/v) as appropriate for the ligands **10**, **11**, **15**, and **16**. Control experiments with histamine, dissolved in double-distilled water or dissolved in a solvent containing 50% (v/v) DMSO and 50% (v/v) double-distilled water, showed that a final DMSO concentration of 5% (v/v) did not shift pK_i and pEC_{50} values of histamine.

Pharmacological and Biochemical Methods. Construction of baculoviruses was described previously (Kelley et al., 2001; Seifert et al., 2003; Straßer et al., 2008a). Cell culture, membrane preparation and determination of protein concentration were performed as described previously (Seifert et al., 2003; Straßer et al., 2008a). [^{3}H]Mepyramine competition binding assay and steady-state GTPase assay were performed as described previously (Kelley et al., 2001; Straßer et al., 2008a). All assays for comparison of pharmacological data were carried out under the same experimental conditions and in parallel. For data analysis the software Prism 4.02 (GraphPad Software Inc., San Diego, CA) was used. pK_i and pK_B values were calculated according to Cheng and Prusoff (1973). All data are the means ± S.E.M. of at least three independent experiments. For comparison of two pairs of data, the significance of the deviation of zero p was calculated using the t test.

Construction of Active H_1R Models with Phenoprodifen 13, Phenylhistamine 9, and Imidazolypropylguanidine 19 in the Binding Pocket. The active state gpH_1R and hH_1R homology models were developed on the basis of the new crystal structure of the human β_2-adrenergic receptor (hβ_2AR) (Cherezov et al., 2007; Rasmussen et al., 2007; Rosenbaum et al., 2007). Both models were constructed as described previously (Straßer et al., 2008b) using restrained molecular dynamics simulations and considering experimental data of activated GPCRs (Niv et al., 2006). Based on the active state models of H_1Rs, ligands **9**, **13**, and **19** were docked manually, and further MD simulations were carried out. The equilibration phase and the productive phase were performed as described previously (Straßer et al., 2008a). For all MD simulations, the software package GROMACS 3.3.1 (http://www.gromacs.org/)

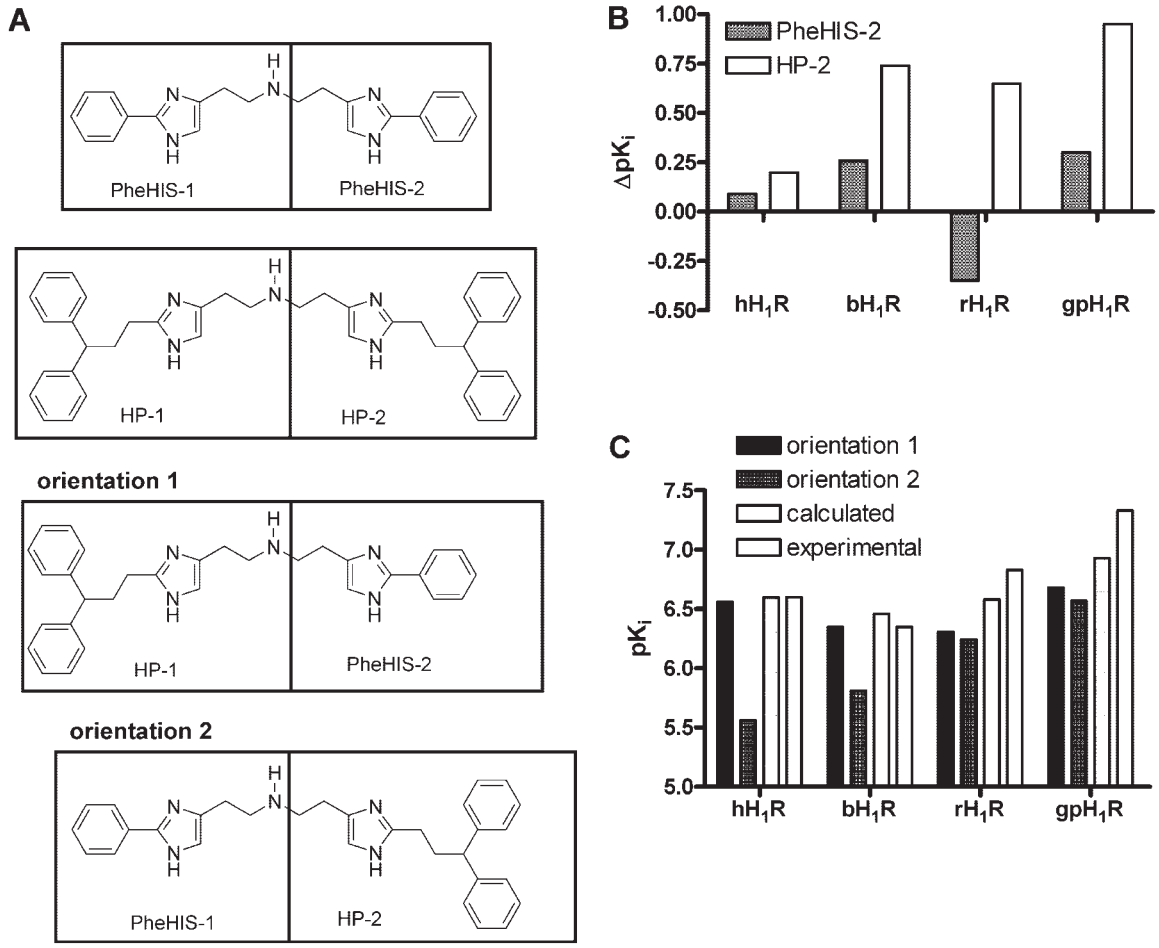

Fig. 2. Relative affinities of phenoprodifens compared with histaprodifen or the corresponding phenylhistamine, respectively. A, partial structures of dimeric phenylhistamine, dimeric histaprodifen, phenoprodifen in orientation 1 and phenoprodifen in orientation 2. B, ΔpK_i values for the moieties PheHIS-2 and HP-2. C, predicted pK_i values for phenoprodifen in orientations 1 and 2 as well as the calculated (including orientations 1 and 2) pK_i values and the experimental ones.

was used in combination with the ffG53A6 force field (Oostenbrink et al., 2004). The force field parameters for the bromine-substituted phenylhistamine **9**, phenoprodifen **13**, and imidazolylpropylguanidine **19** were adopted from the ffG53A6 force field. The electrostatic potential surface was calculated with Sybyl 7.0 (Tripos, St. Louis, MO) based on Gasteiger-Hückel partial charges. For multifit alignment of phenylhistamine **9** and imidazolylpropylguanidine **19**, Sybyl 7.0 was used.

Model to Predict the Orientation of the Unsubstituted Phenoprodifen 13. To analyze the question of orientation of the unsubstituted phenoprodifen **13**, we implemented the model illustrated in Fig. 2. The dimeric phenylhistamine **10** and dimeric histaprodifen **17** were divided into the parts PheHIS-1, PheHIS-2, HP-1, and HP-2, respectively (Fig. 2A). The moieties PheHIS-1 and HP-1 were related to the phenylhistamine **2** and histaprodifen **12**, respectively, with regard to their pK_i values, which represent the $\log_{10}$ of the association constants of the receptor-ligand-complexes. The ΔpK_i values of the moieties PheHIS-2 and HP-2 (Fig. 2B) were calculated by pK_i(**10**) − pK_i(**2**) and pK_i(**17**) − pK_i(**12**). Subsequently, the pK_i value of the phenoprodifen **13** was calculated by pK_i (orientation 1) = pK_i(**12**) + ΔpK_i(PheHIS-2) in case of orientation 1 and by pK_i (orientation 2) = pK_i(**2**) + ΔpK_i(HP-2) in case of orientation 2. The term $10^{pK_i(\text{orientation 1})}/10^{pK_i(\text{orientation 2})}$ corresponds to the ratio concentration (orientation 1)/concentration (orientation 2). For calculation of pK_i values, including orientation 1 and orientation 2, the equation $\log_{10}[K_i \text{ (orientation 1)} + K_i \text{ (orientation 2)}]$ was used.

Results

Analysis of Phenylhistamines and Phenoprodifens at H_1R Species Isoforms in the [^{3}H]Mepyramine Competition Binding Assay. The affinities of the compounds determined in the competition binding assay are given in Table 1. At hH_1R and bH_1R, the affinity of phenylhistamine **2** was lower than for histamine **1**, but at rH_1R and gpH_1R, the affinity for **2** was in the same range as for **1**. The introduction of an additional methyl group in phenylhistamines in *S*-configuration (**3S**) showed no significant difference compared with the unmethylated compound **2**. However, a significant decrease in pK_i values was observed for compound **3R** with the additional methyl group in *R*-configuration. The introduction of a trifluoromethyl group in *meta* position into the phenyl moiety of the phenylhistamine **4** led to an increase of approximately 0.5–0.7 in pK_i values compared with the unsubstituted phenylhistamine **2** at all four species isoforms. The *S*-enantiomer **5S** showed the same affinity as the unmethylated derivative **4** at hH_1R, bH_1R, rH_1R and gpH_1R. However, there was a significant decrease ($p < 0.001$ at hH_1R and bH_1R, $p < 0.01$ at rH_1R, $p < 0.0001$ at gpH_1R) of approximately 1 unit in pK_i of the *R*-enantiomer **5R** compared with the *S*-enantiomer **5S** at all four species isoforms. The exchange of the trifluoromethyl group to bromine **6** did not reveal significant differences in affinities of **6** compared with **4** at hH_1R, bH_1R, rH_1R, and gpH_1R.

The affinities of phenylhistamine **7** showed no significant differences at hH_1R, bH_1R, and rH_1R, but at gpH_1R, the pK_i of **7** was significantly lower than of **2** ($p < 0.05$). There was no significant difference in affinities of **7** among all four species isoforms. The pK_i values of the bulky trifluoromethylated phenylhistamine **8** compared with the small trifluoromethylated phenylhistamine **4** showed a significant decrease at gpH_1R ($p < 0.001$). The affinities of **8** at hH_1R and rH_1R on the one hand and at bH_1R and gpH_1R on the other hand were not significantly different from one another, but the affinities of **8** were significantly higher at hH_1R and rH_1R compared with bH_1R and gpH_1R ($p < 0.0002$). The pK_i values of the bromine-substituted bulky phenylhistamine **9** compared with the bromine-substituted phenylhistamine **6** showed a significant increase at hH_1R ($p < 0.02$), no significant difference at bH_1R and rH_1R, but a significant decrease at gpH_1R ($p < 0.02$). The affinities of **9** (Fig. 3A) at hH_1R and rH_1R on the one hand and at bH_1R and gpH_1R on the other hand were not significantly different from one another, but the affinities of **9** were higher at hH_1R and rH_1R compared with bH_1R and gpH_1R.

The affinities of the dimeric phenylhistamine **10** were in the same range as for the monomeric phenylhistamine **2** at all four species isoforms. The trifluoromethylated phenylhistamine **11** showed affinities comparable with those of **10**.

The introduction of an additional methyl group into phenoprodifen **13** led to the chiral phenoprodifens **14R** and **14S** showing lower affinities than **13** at all four species isoforms (Straßer et al., 2008a). The trifluoromethyl- substituted (**15**) and bromine-substituted (**16**) phenoprodifens showed a decrease in affinity at all four species isoforms, compared with the unsubstituted phenoprodifen **13**. Moreover, the affinities of **15** and **16** increased in the series $bH_1R < hH_1R < rH_1R < gpH_1R$. The affinities of dimeric histaprodifen **17** were in a range comparable to that found for phenoprodifen **13** or slightly higher.

Analysis of Phenylhistamines and Phenoprodifens at H_1R Species Isoforms in the Steady-State GTPase Assay. The potencies and efficacies of phenylhistamines and phenoprodifens determined in the steady-state GTPase assay are given in Table 2. Compared with histamine **1**, phenylhistamine **2** showed a significantly lower potency at hH_1R and bH_1R, but at rH_1R and gpH_1R, the potencies of **2** and **1** were

TABLE 1

Affinities of histamine, phenylhistamines, and phenoprodifens at hH_1R, bH_1R, rH_1R, and gpH_1R coexpressed with RGS4 in Sf9 cell membranes in the competition binding assay

[^{3}H]Mepyramine competition binding in Sf9 membranes expressing hH_1R, bH_1R, rH_1R, and gpH_1R in combination with RGS4 was determined in presence of 5 nM [^{3}H]mepyramine as described under *Materials and Methods*. Data were analyzed by nonlinear regression and were best fit to one-site (monophasic) competition curves. pK_i values were calculated according to Cheng and Prusoff (1973). Data shown are the means ± S.E.M. of at least three experiments with independent membrane preparations each performed in duplicate.

Compound	pK_i			
	hH_1R	bH_1R	rH_1R	gpH_1R
1[a]	5.62 ± 0.03	5.93 ± 0.10	5.43 ± 0.03	5.50 ± 0.03
2	5.36 ± 0.13	5.07 ± 0.08	5.59 ± 0.24	5.62 ± 0.05
3R	4.50 ± 0.02	4.60 ± 0.12	4.94 ± 0.14	4.70 ± 0.09
3S	5.17 ± 0.10	5.44 ± 0.21	5.33 ± 0.08	5.45 ± 0.10
4	5.83 ± 0.10	5.71 ± 0.17	6.13 ± 0.05	6.32 ± 0.01
5R	4.90 ± 0.07	4.83 ± 0.09	4.89 ± 0.23	5.20 ± 0.02
5S	5.95 ± 0.07	5.99 ± 0.08	6.13 ± 0.12	6.17 ± 0.04
6	5.86 ± 0.09	5.67 ± 0.03	6.10 ± 0.12	6.26 ± 0.17
7	5.38 ± 0.07	5.20 ± 0.04	5.39 ± 0.23	5.28 ± 0.10
8	6.14 ± 0.03	5.27 ± 0.01	6.28 ± 0.10	5.36 ± 0.06
9	6.43 ± 0.08	5.76 ± 0.12	6.33 ± 0.11	5.46 ± 0.15
10	5.45 ± 0.17	5.33 ± 0.07	5.24 ± 0.03	5.92 ± 0.08
11	5.66 ± 0.06	5.42 ± 0.07	5.50 ± 0.10	5.94 ± 0.10
12[a]	6.47 ± 0.11	6.09 ± 0.10	6.66 ± 0.13	6.38 ± 0.11
13[a]	6.60 ± 0.07	6.35 ± 0.12	6.83 ± 0.36	7.33 ± 0.08
14R[a]	6.08 ± 0.06	6.08 ± 0.40	6.49 ± 0.15	6.74 ± 0.02
14S[a]	6.40 ± 0.15	5.83 ± 0.03	5.98 ± 0.20	6.38 ± 0.17
15	6.48 ± 0.07	6.33 ± 0.06	6.51 ± 0.12	6.65 ± 0.15
16	5.91 ± 0.15	5.84 ± 0.04	6.31 ± 0.17	6.47 ± 0.14
17[a]	6.67 ± 0.01	6.83 ± 0.26	7.31 ± 0.10	7.33 ± 0.14

[a] Data were taken from Straßer et al. (2008a) and were obtained in parallel with the compounds presented in this study.

in a comparable range. The efficacy of phenylhistamine **2** increased in the series $hH_1R < bH_1R < rH_1R < gpH_1R$ from 72 to 92% relative to histamine. The introduction of an additional methyl group in *S*-configuration (**3S**) and in *R*-configuration (**3R**) led to slight and large decreases in potency, respectively, compared with **2** at all four species isoforms. In addition, a decrease in efficacy in a range from approximately 34 to 56% for **3S** and **3R** compared with **2** at hH_1R, bH_1R, rH_1R, and gpH_1R was observed. The trifluoromethylated phenylhistamine **4** showed an increase in potency but a decrease in efficacy compared with **2** at all four species isoforms. The introduction of a methyl group in *S*-configuration **5S** led to a slight decrease in potency compared with **4**, but in case of *R*-configuration **5R**, the decrease in potency was significant in the range of approximately 1 log unit compared with **4**. The efficacy of the chiral trifluoromethylated phenylhistamines **5R** and **5S** were decreased significantly compared with **4** at hH_1R, bH_1R, and rH_1R, but at gpH_1R no decrease was observed. The exchange of the trifluoromethyl group against a bromine in compound **6** led to a slight increase in potency compared with **4**. The efficacies of **6** compared with **4** were in the same range at hH_1R and bH_1R, but increased at rH_1R and gpH_1R. In general, the potencies of all small phenylhistamines **2**-**6** were more similar between

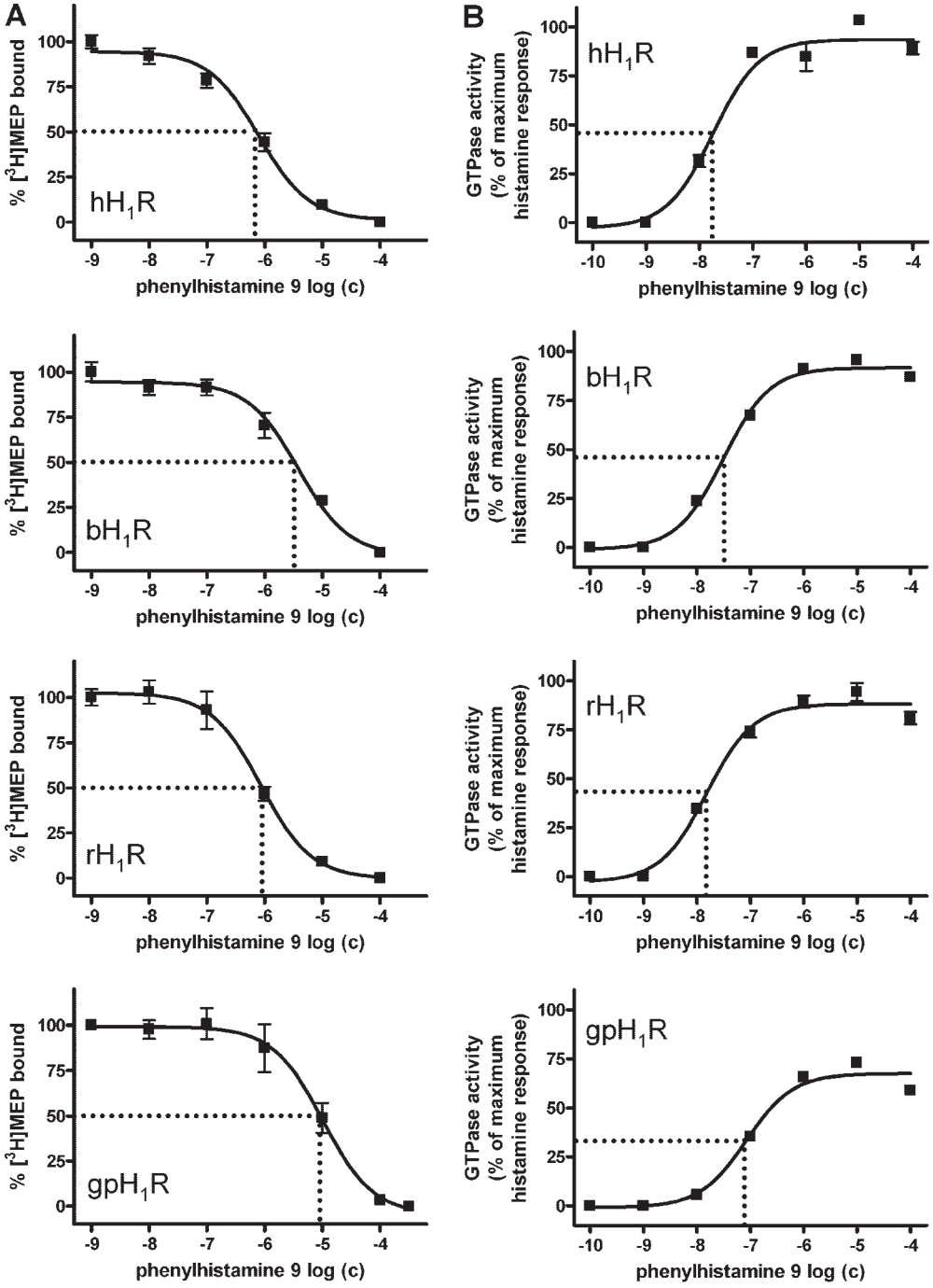

Fig. 3. Competition binding isotherms and concentration-response curves for the bulky bromine-substituted phenylhistamine **9** at hH_1R, bH_1R, rH_1R, and gpH_1R. The experiments were performed using Sf9 cell membranes expressing hH_1R, bH_1R, rH_1R, or gpH_1R and RGS4 as described under *Materials and Methods*. Data were analyzed by nonlinear regression and were best fit to one-site (monophasic) competition curves. A, competition binding isotherms; the experiments were performed in presence of 5 nM [^{3}H]-mepyramine ([^{3}H]MEP). B, concentration response curves determined in the steady-state GTPase assay.

hH_1R and bH_1R on the one hand and between rH_1R and gpH_1R on the other hand, with higher potencies at rH_1R and gpH_1R.

All small phenylhistamines act as partial agonists at hH_1R, bH_1R, rH_1R, and gpH_1R. The introduction of a trifluoromethyl group or bromine in *meta* position of the terminal phenyl moiety increased affinity as well as potency at all four species isoforms. The introduction of an additional methyl group in α-position significantly reduced efficacy for both enantiomers. At all four species isoforms, the *S*-enantiomer showed higher affinity and potency than the *R*-enantiomer. Based on these results, it can be concluded that the phenylhistamines with the additional methyl group do not fit optimally into the binding pocket of the receptors and that the methyl group in *R*-configuration is more disfavored than the methyl group in *S*-configuration. Moreover, as shown by the decrease in efficacy this additional methyl group seems to hinder the activation process of the receptor independently of the configuration. The conformational change of the aromatic motif $Phe^{6.52}$, $Trp^{6.48}$, and $Phe^{6.44}$ (Straßer and Wittmann, 2007) probably cannot be fully established because of sterical hindrance.

The bulky phenylhistamines **7** to **9** were partial agonists at all four species isoforms. Compared with the corresponding phenylhistamines **2**, **4**, and **6**, the potency was significantly higher at hH_1R and bH_1R, comparable at rH_1R, but significantly lower at gpH_1R. At all four species isoforms, the potency increased in the series **7** < **8** < **9**. The highest potencies were found for the bromine-substituted phenylhistamine **9** (Fig. 3B) in a pEC_{50} range from 7 to 8, with a significant increase in potency in the series $gpH_1R < bH_1R < hH_1R \approx rH_1R$. The phenylhistamines **7** to **9** showed a significantly higher potency at hH_1R that at gpH_1R; thus, we have identified the first phenylhistamine derivatives with a higher potency at hH_1R compared with gpH_1R. The efficacies of **7** to **9** are comparable (approximately 90%) at hH_1R, bH_1R, and rH_1R but significantly lower (approximately 70%) at gpH_1R.

The dimeric phenylhistamines **10** and **11** were partial agonists with potencies in the range of approximately 5.5–6.5 at all four species isoforms. The potency as well as the efficacy of the trifluoromethylated derivative **11** was higher than the potency and efficacy of the unsubstituted and symmetrical dimeric phenylhistamine **10** at all four species isoforms.

Histaprodifen **12**, the unsubstituted phenoprodifen **13**, chiral phenoprodifens **14R** and **14S**, and dimeric histaprodifen **17** were analyzed in a previous study (Straßer et al., 2008a). In this study, we completed the pharmacological characterization of the phenoprodifens, including the trifluoromethylated **15** and bromine-substituted phenoprodifen **16**. In contrast to the chiral phenoprodifens **14R** and **14S**, the compounds **15** and **16** are partial agonists at all four species isoforms, as well as phenoprodifen **13** itself. The potency of **15** and **16** were in the same range as for **13** at hH_1R and bH_1R, but at rH_1R and at gpH_1R, an increase and a decrease in potency, respectively, were observed. Dimeric histaprodifen **17**, acting as a partial agonist at all four species isoforms, exhibits potencies in the same range, as phenoprodifen **13**.

Analysis of Phenylhistamines 7, 8, and 9 at hH_2R-$G_s\alpha_S$ in the Steady-State GTPase Assay. To determine whether **7**, **8**, and **9**, showing selectivity for hH_1R relative to gpH_1R, also exhibit selectivity relative to the hH_2R, we analyzed the compounds in the GTPase assay using the hH_2R-$G_s\alpha_S$ fusion protein. The potencies of phenylhistamines **7**, **8**, and **9** determined at hH_2R-$G_s\alpha_S$ showed a significant decrease of approximately 1 log unit compared with the potencies at hH_1R (Table 3). As they were at hH_1R, **7**, **8**, and **9** were partial agonists at hH_2R-$G_s\alpha_S$. The efficacy of phenylhistamines **7** and **9** was significantly reduced at hH_2R-$G_s\alpha_S$ relative to hH_1R, but for the trifluoromethyl-substituted phenylhistamine **8**, there was no significant difference in efficacy between hH_1R and hH_2R-$G_s\alpha_S$. The imidazolylpropylguanidine (UR-AK57) **19** (Xie et al., 2006) acts as partial agonist at hH_1R and hH_2R-$G_s\alpha_S$, as well as the phenylhistamines **7**, **8**,

TABLE 2

Potencies and efficacies of histamine, phenylhistamines, and phenoprodifens at hH_1R, bH_1R, rH_1R, and gpH_1R coexpressed with RGS4 in Sf9 cell membranes in the steady-state GTPase assay

All GTPase experiments were performed as described under *Materials and Methods*. Data were analyzed by nonlinear regression and were best fit to sigmoidal concentration-response curves. The efficacy (E_{max}) of histamine was set at 1.00. The E_{max} values of all other compounds were referred to this value. Data shown are means ± S.E.M. of at least three experiments were each performed in duplicate or triplicate. Membranes were used from independent membrane preparations.

Compound	hH_1R		bH_1R		rH_1R		gpH_1R	
	pEC_{50}	E_{max}	pEC_{50}	E_{max}	pEC_{50}	E_{max}	pEC_{50}	E_{max}
1[a]	6.92 ± 0.07	1.00	6.86 ± 0.16	1.00	6.59 ± 0.13	1.00	6.69 ± 0.10	1.00
2	6.14 ± 0.06	0.72 ± 0.04	6.18 ± 0.04	0.82 ± 0.02	6.89 ± 0.06	0.84 ± 0.07	6.96 ± 0.02	0.92 ± 0.08
3R	5.24 ± 0.10	0.23 ± 0.01	5.23 ± 0.14	0.33 ± 0.09	5.76 ± 0.09	0.50 ± 0.06	5.84 ± 0.09	0.51 ± 0.06
3S	5.84 ± 0.01	0.21 ± 0.01	5.99 ± 0.16	0.26 ± 0.03	6.31 ± 0.05	0.43 ± 0.08	6.38 ± 0.11	0.58 ± 0.04
4	6.71 ± 0.04	0.61 ± 0.02	6.77 ± 0.08	0.65 ± 0.03	7.25 ± 0.20	0.76 ± 0.07	7.28 ± 0.08	0.66 ± 0.05
5R	5.85 ± 0.16	0.23 ± 0.01	5.70 ± 0.08	0.32 ± 0.01	6.05 ± 0.10	0.53 ± 0.05	6.19 ± 0.14	0.60 ± 0.02
5S	6.58 ± 0.02	0.21 ± 0.01	6.48 ± 0.09	0.31 ± 0.01	6.85 ± 0.10	0.42 ± 0.07	7.06 ± 0.13	0.56 ± 0.04
6	6.75 ± 0.03	0.62 ± 0.01	6.93 ± 0.01	0.68 ± 0.02	7.59 ± 0.10	0.87 ± 0.03	7.42 ± 0.09	0.82 ± 0.03
7	6.45 ± 0.02	0.92 ± 0.03	6.49 ± 0.01	0.89 ± 0.01	6.70 ± 0.06	0.90 ± 0.04	6.10 ± 0.05	0.64 ± 0.01
8	7.48 ± 0.02	0.93 ± 0.04	7.26 ± 0.04	0.92 ± 0.04	7.48 ± 0.03	0.94 ± 0.04	6.81 ± 0.03	0.73 ± 0.03
9	7.75 ± 0.11	0.94 ± 0.06	7.50 ± 0.04	0.92 ± 0.03	7.82 ± 0.08	0.91 ± 0.04	7.08 ± 0.07	0.68 ± 0.03
10	5.63 ± 0.07	0.26 ± 0.01	5.45 ± 0.10	0.25 ± 0.02	6.00 ± 0.04	0.55 ± 0.01	5.98 ± 0.11	0.20 ± 0.05
11	6.18 ± 0.07	0.51 ± 0.05	5.96 ± 0.11	0.45 ± 0.02	6.63 ± 0.01	0.72 ± 0.01	6.46 ± 0.19	0.40 ± 0.04
12[a]	6.95 ± 0.06	0.62 ± 0.07	7.00 ± 0.11	0.67 ± 0.03	7.36 ± 0.16	0.82 ± 0.06	7.50 ± 0.09	0.74 ± 0.04
13[a]	6.67 ± 0.08	0.52 ± 0.05	6.68 ± 0.03	0.57 ± 0.14	6.50 ± 0.08	0.75 ± 0.07	7.25 ± 0.16	0.79 ± 0.05
14R[a]	6.56 ± 0.15 (pK_B)		5.93 ± 0.06 (pK_B)		5.86 ± 0.11 (pK_B)		7.20 ± 0.22	0.60 ± 0.10
14S[a]	6.61 ± 0.11 (pK_B)		6.06 ± 0.16 (pK_B)		6.08 ± 0.06 (pK_B)		7.09 ± 0.09	0.23 ± 0.03
15	6.45 ± 0.07	0.55 ± 0.02	6.49 ± 0.03	0.49 ± 0.03	7.16 ± 0.04	0.64 ± 0.04	6.82 ± 0.01	0.69 ± 0.01
16	6.57 ± 0.08	0.45 ± 0.01	6.56 ± 0.03	0.44 ± 0.01	6.95 ± 0.06	0.69 ± 0.02	6.83 ± 0.01	0.58 ± 0.02
17[a]	6.18 ± 0.12	0.65 ± 0.11	6.73 ± 0.13	0.71 ± 0.15	6.90 ± 0.05	0.58 ± 0.07	7.18 ± 0.18	0.92 ± 0.08

[a] Data were taken from Straßer et al. (2008a) and were obtained in parallel with the compounds presented in this study.

and **9**. The potency of **19** is comparable with the potency of **7** at hH_1R. But at $hH_2R\text{-}G_s\alpha_S$, the potency of **19** is higher than that of **7**, **8**, and **9**.

Binding Mode of Phenoprodifen Based on Molecular Dynamics Simulations. In a previous study, we showed that suprahistaprodifen can bind to the H_1R in two different orientations (Straßer et al., 2008a). Likewise, the molecular dynamics simulations at hH_1R and gpH_1R led to stable ligand-receptor complexes for the phenoprodifens **13** to **16** in both orientations (Fig. 4, A and B, for **13**) in the binding pocket. The positively charged amine moiety in the center of the phenoprodifens interacts electrostatically with the highly conserved, negatively charged $Asp^{3.32}$ and $Tyr^{7.43}$ (not shown in Fig. 4 to preserve clarity). In both orientations, one imidazole moiety forms stable hydrogen bonds to $Ser^{3.36}$ and $Tyr^{6.51}$, the second imidazole moiety forms stable hydrogen bonds to a conserved Glu (Glu-181 in hH_1R, Glu-190 in gpH_1R) in the second extracellular loop and $Trp^{7.40}$. These interactions are similar to those described for the dimeric histaprodifen in a prior study (Straßer et al., 2008b). The terminal phenyl moiety and the diphenylpropyl group, respectively, are embedded into hydrophobic pockets determined by $Leu^{1.35}$, $Leu^{1.39}$, $Leu^{2.65}$, $Trp^{3.28}$, and $Ile^{3.40}$ (not shown in Fig. 4 for clarity) and $Trp^{6.48}$.

The highly conserved $Trp^{6.48}$ is involved in the rotamer toggle switch during the process of receptor activation (Crocker et al., 2006). Our simulations reproducibly showed that $Trp^{6.48}$ was in a stable conformation parallel to the lipid bilayer, as described for the activate conformation of a GPCR (Straßer and Wittmann, 2007), only for the phenoprodifens bound in orientation 2. In orientation 1, the planar conformation of $Trp^{6.48}$ was unstable in every simulation and switched back into an almost vertical conformation with regard to the lipid bilayer, but all other characteristics for the active state were conserved.

Prediction of the Orientation of Phenoprodifen 13. The predicted pK_i values for phenoprodifen in orientations 1 and 2 are summarized in Fig. 2C and Table 4, respectively. The data show that orientation 1 is clearly preferred at hH_1R and bH_1R, but at rH_1R and gpH_1R, neither orientation 1 nor orientation 2 is preferred. The calculated pK_i value reflects the fact that phenoprodifen binds in both orientations. A comparison of the predicted pK_i values (including orientations 1 and 2) with the experimental ones shows a very good correlation between prediction and experiment at all four species isoforms.

Interaction Energy of Phenoprodifen 13 with hH_1R and gpH_1R. In Fig. 5, the interaction energy of phenoprodifen **13** in orientation 1 and orientation 2, respectively, with hH_1R and gpH_1R is calculated for 1 ns of simulation time during the equilibrated productive phase. The interaction energy of phenoprodifen **13** with hH_1R (Fig. 5A) is significantly different ($p < 0.025$) between orientation 1 [$\Delta E(hH_1R\text{-}\mathbf{13}) = -549 \pm 22$ kJ/mol] and orientation 2 [$\Delta E(hH_1R\text{-}\mathbf{13}) = -471 \pm 30$ kJ/mol]. In contrast, the mean interaction energy between ligand and receptor is not significantly different at gpH_1R (Fig. 5B) in orientations 1 [$\Delta E(gpH_1R\text{-}\mathbf{13}) = -613 \pm 33$ kJ/mol] and 2 [$\Delta E(gpH_1R\text{-}\mathbf{13}) = -589 \pm 21$ kJ/mol].

Binding Mode of Bulky Phenylhistamines Based on Molecular Dynamics Simulations. Docking studies and extensive molecular dynamics simulations with the bulky phenylhistamines in the active state model of hH_1R and gpH_1R, respectively, revealed four possible binding modes. In binding modes 1 (Fig. 6A) and 2 (Fig. 6B), the bulky phenylhistamines are bound similarly to the phenylhistamine-histamine partial structure of the phenoprodifen in orientations 1 (Fig. 4A) and 2 (Fig. 4B). However, we observed a very high flexibility of the terminal histamine moiety in both orientations because the stabilization with the second diphenylpropyl moiety is lost. The third binding mode identified is very different from binding modes 1 and 2. Compared with binding mode 2, the whole ligand is shifted to the left in direction of transmembrane helix 5, with the following consequences. First, the hydrogen bond between the terminal histamine moiety and $Ser^{3.36}$ is broken. Second, a new hydrogen bond between the terminal histamine moiety and $Lys^{5.39}$ is formed in analogy to the binding mode described for histamine (Fig. 6C). However, because of the high flexibility of the terminal histamine moiety, the hydrogen bond to $Lys^{5.39}$ was not observed during the entire simulation time. In binding mode 4, the terminal histamine moiety established a stacked aromatic interaction with $Tyr^{3.33}$ and to the hydroxyl moiety of

TABLE 3

Potencies and efficacies of phenylhistamines **7**, **8**, and **9** at hH_1R coexpressed with RGS4 and at $hH_2R\text{-}G_s\alpha_S$ expressed in Sf9 cell membranes in the steady-state GTPase assay and comparison with imidazolylpropylguanidine **19**

Steady-state GTPase activity in Sf9 cell membranes expressing hH_1R and RGS4 or $hH_2R\text{-}G_{s\alpha S}$ was determined as described under *Materials and Methods*. Data were analyzed by nonlinear regression and were best fit to sigmoidal concentration-response curves. The efficacy (E_{max}) of histamine was set 1.00. The E_{max} values of all other compounds were referred to this value. Data shown are means ± S.E.M. of at least three experiments, each performed in duplicate. Membranes were used from independent membrane preparations.

Compound	hH_1R		$hH_2R\text{-}G_{s\alpha S}$	
	pEC_{50}	E_{max}	pEC_{50}	E_{max}
7	6.45 ± 0.02	0.92 ± 0.03	5.19 ± 0.02	0.46 ± 0.01
8	7.47 ± 0.02	0.93 ± 0.04	6.13 ± 0.08	0.82 ± 0.05
9	7.75 ± 0.11	0.94 ± 0.06	6.60 ± 0.04	0.18 ± 0.05
19[a]	6.55 ± 0.01	0.56 ± 0.06	7.64 ± 0.05	0.87 ± 0.05

[a] Data were taken from Xie et al. (2006).

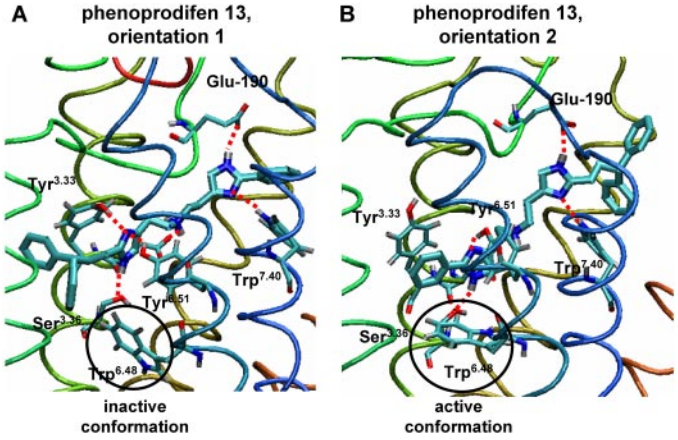

Fig. 4. Binding mode of phenoprodifen **13** at gpH_1R. A, stable conformation of phenoprodifen **13** in the binding pocket of gpH_1R, observed in MD simulations in orientation 1. B, stable conformation of phenoprodifen **13** in the binding pocket of gpH_1R, observed in MD simulations in orientation 2. The MD-simulations were performed as described under *Materials and Methods*. Hydrogen bonds and electrostatic interaction between ligand and amino acids are marked as red dashed lines. At hH_1R, binding modes of phenoprodifen **13** were similar to the modes at gpH_1R. The amino acids of the transmembrane domains are numbered concerning to the nomenclature of Ballesteros et al. (2001).

Tyr$^{6.51}$ (Fig. 6D). The bromine of phenylhistamine **9** is located near Ser$^{2.61}$ in gpH_1R and Asn$^{2.61}$ in hH_1R, respectively. However, there is a gap between the bromine and Ser$^{2.61}$ (Fig. 6E), but a close contact between bromine and Asn$^{2.61}$ (Fig. 6F). The distance between the bromine of **9** and Ser$^{2.61}$ in gpH_1R is approximately 3.5 Å and between the bromine of **9** and Asn$^{2.61}$ in hH_1R is approximately 2.6 Å. Thus, the van der Waals and electrostatic interaction between bromine and Asn$^{2.61}$ is more effective than between bromine and Ser$^{2.61}$.

Discussion

Pharmacological Differences of Bulky Phenylhistamines and Phenoprodifens at hH_1R, bH_1R, rH_1R, and gpH_1R. It has been assumed that, as a general rule, synthetic agonists exhibit higher potency and efficacy at gpH_1R than at hH_1R (Seifert et al., 2003; Straßer et al., 2008a). However, as a notable exception, the imidazolylpropylguanidine **19** (UR-AK57), originally designed as a selective H_2R agonist, exhibits higher potency and efficacy as hH_1R-agonist than as gpH_1R-agonist (Xie et al., 2006).

In this study, we analyzed 11 new phenylhistamines and phenoprodifens at four H_1R species isoforms. Compared with the small phenylhistamines, the larger phenylhistamines **7**, **8**, and **9** exhibited a completely different pharmacological profile at hH_1R, bH_1R, rH_1R, and gpH_1R. The affinities and potencies of these compounds are, in general, higher at hH_1R and rH_1R compared with gpH_1R, whereas bH_1R shows values between those for hH_1R and rH_1R on the one hand and for gpH_1R on the other hand. Thus, we have identified the first phenylhistamines with higher affinity at hH_1R than at gpH_1R. The differences $pK_i(hH_1R)$-$pK_i(gpH_1R)$ or pEC_{50}-(hH_1R)-$pEC_{50}(gpH_1R)$ are positive and significantly higher for the trifluoromethylated **8** or bromine-substituted **9** phenylhistamine than for the unsubstituted phenylhistamine **7**. Molecular dynamics simulations revealed a very different binding mode of the phenylhistamines compared with that of the phenoprodifens. Compared with the histamine moiety of the phenoprodifen, the terminal histamine moiety of the phenylhistamine is shifted to the left near transmembrane helix 5. The hydrogen bond between the imidazole moiety and Ser$^{3.36}$ is lost. Instead, the imidazole moiety establishes a new hydrogen bond to Lys$^{5.39}$ (Fig. 6C). Thus, the binding mode of this terminal histamine moiety is very similar to the binding mode described for histamine (Jongejan et al., 2005). The trifluoromethyl group or the bromine of **8** and **9**, respectively, are in close contact to Asn$^{2.61}$ in the case of hH_1R (Fig. 6F) and to Ser$^{2.61}$ in the case of gpH_1R (Fig. 6E). Asn$^{2.61}$ is a selectivity switch between hH_1R and gpH_1R (Bruysters et al., 2005). Based on the simulation studies, it can be proposed that this amino acid difference between hH_1R and gpH_1R is important for the observed species differences. However, because the affinity and potency of **8** and **9** at bH_1R (Asn$^{2.61}$) are different from those of hH_1R (Asn$^{2.61}$) and rH_1R (Asn$^{2.61}$)

TABLE 4

Model to predict the orientation of the unsubstituted phenoprodifen **13**

The experimental binding affinities of phenylhistamine **2**, dimeric phenylhistamine **10**, histaprodifen **12**, and dimeric histaprodifen **17** were used to predict the binding affinities of phenoprodifen **13** in orientations 1 and 2 at hH_1R, bH_1R, rH_1R, and gpH_1R. Calculations were performed as described under *Materials and Methods*.

	Calculation	hH_1R	bH_1R	rH_1R	gpH_1R
PheHIS-1[a]	pK_i (**2**)	5.36	5.07	5.59	5.62
PheHIS-2[b]	pK_i (**10**) − pK_i (**2**)	0.09	0.26	−0.35	0.30
HP-1[a]	pK_i (**12**)	6.47	6.09	6.66	6.38
HP-2[b]	pK_i (**17**) − pK_i (**12**)	0.20	0.74	0.65	0.95
pK_i (13, orientation 1)[c]	HP-1 + PheHIS-2	6.56	6.35	6.31	6.68
pK_i (13, orientation 2)[c]	PheHIS-1 + HP-2	5.56	5.81	6.24	6.57
pK_i (calculated)[c]	$\log_{10}(K_i$ (**13**, orientation 1) + K_i (**13**, orientation 2))	6.60	6.46	6.58	6.93

[a] pK_i values, measured.
[b] Differences in pK_i values.
[c] Estimated.

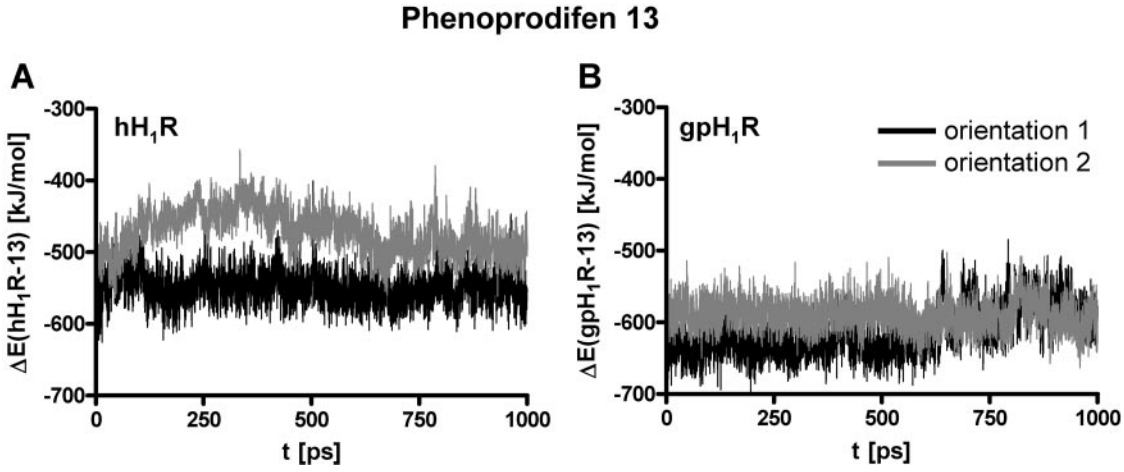

Fig. 5. Interaction energy of phenoprodifen **13** with hH_1R and gpH_1R in orientations 1 and 2. The interaction energy of phenoprodifen **13** with hH_1R [$\Delta E(hH_1R$-**13**)] and with gpH_1R [$\Delta E(gpH_1R$-**13**)] was calculated during a 1-ns productive phase in MD simulation. At each time step, the potential energy of the receptor and of the ligand were subtracted from the potential energy of the corresponding ligand receptor complex.

on one hand and gpH$_1$R (Ser$^{2.61}$) on the other hand, it is likely that in addition to the Asn$^{2.61}$/Ser$^{2.61}$ mutation, other differences in amino acid sequences contribute to the pharmacological differences as well.

In contrast to the observations made for phenylhistamines, the introduction of a trifluoromethyl group or a bromine into the terminal phenyl moiety of the phenoprodifens did not increase affinity or potency. In a previous study (Straßer et al., 2008b), we have described that the unsubstituted phenoprodifen can bind in two different orientations into the binding pocket of the H$_1$R. In orientation 1, the histaprodifen partial structure is located near TM5, and the phenylhistamine partial structure near TM2. In orientation 2, the phenylhistamine partial structure is located near TM5 and the histaprodifen partial structure near TM2. Further molecular dynamics simulations have shown that the trifluoromethyl-

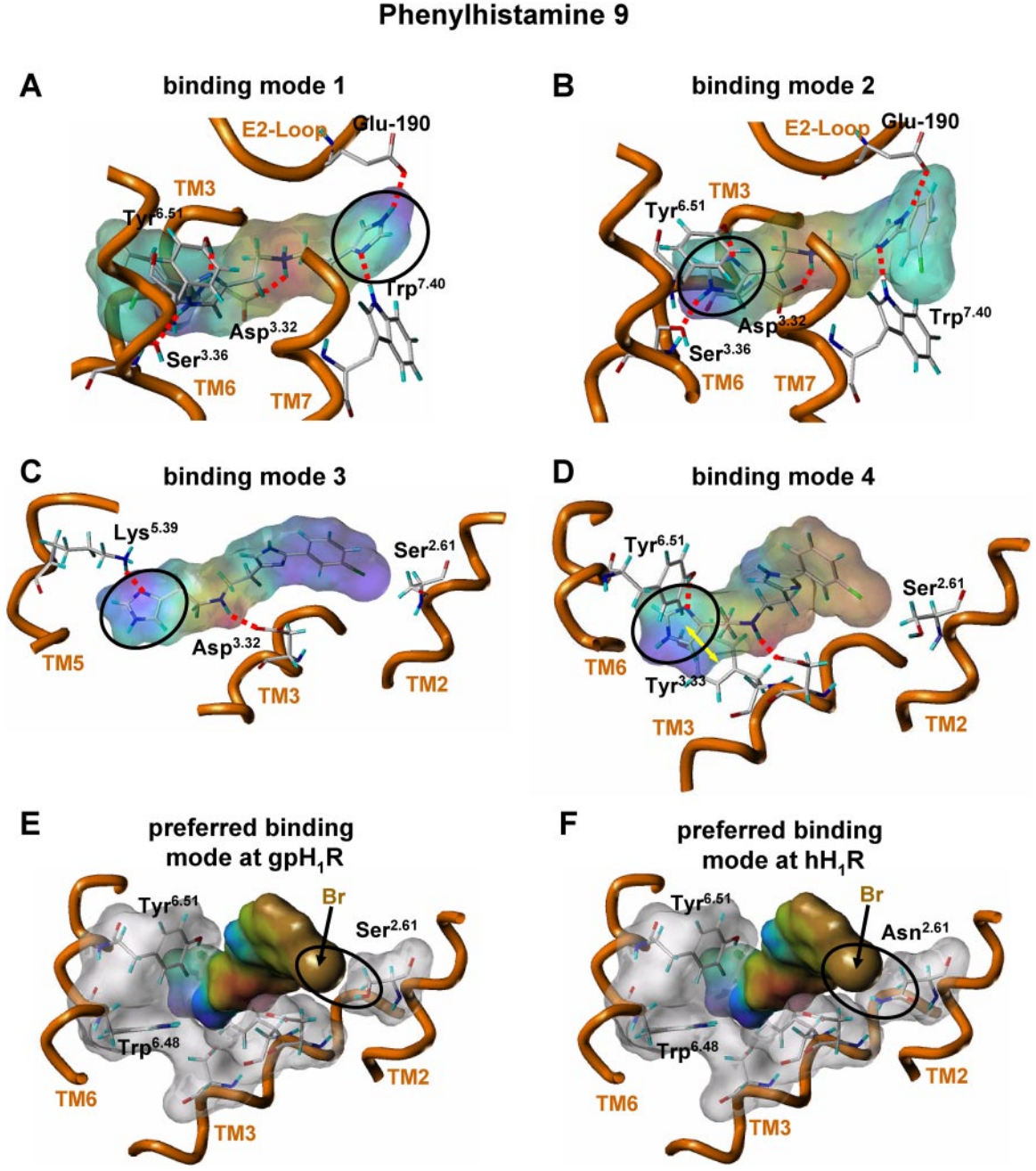

Fig. 6. Binding mode of bulky bromine-substituted phenylhistamine **9** at gpH$_1$R and hH$_1$R. Bromine-substituted phenylhistamine **9** in the binding pocket: A, binding mode 1 at gpH$_1$R. B, binding mode 2 at gpH$_1$R. C, binding mode 3 at gpH$_1$R. D, binding mode 4 at gpH$_1$R, representing the most stable conformation during MD simulation. E, most preferred binding mode of bromine-substituted phenylhistamine **9** in the binding pocket of gpH$_1$R observed in MD simulations. F, most preferred binding mode of bromine-substituted phenylhistamine **9** in the binding pocket of hH$_1$R observed in MD simulations. The MD-simulations were performed as described under *Materials and Methods*. A–D, hydrogen bonds and electrostatic interaction between ligand and amino acids are marked as red dashed lines; the black circle marks the free terminal imidazolyl moiety. D, the yellow arrow indicates a stacked aromatic interaction between the free terminal imidazolyl moiety of **9** and Tyr$^{3.33}$. E and F, for the ligand, the electrostatic potential surface is shown; red indicates positive charge, green and brown indicates nearly neutral regions, blue indicates negative charge. The van der Waals surfaces of the most important amino acid side chains that are interacting with the ligand are given in gray shading. The black circles mark the contact between the bromine and Ser$^{2.61}$ and Asn$^{2.61}$, respectively.

substituted **15** and bromine-substituted **16** phenoprodifens can bind in two different orientations into the binding-pocket, too.

Orientation of Phenoprodifen 13 and the Role of the $Trp^{6.48}$ in the Binding of Phenoprodifen 13. Phenoprodifen **13** acts as a partial agonist (Table 2) at hH_1R and gpH_1R. Thus, it can be proposed that the binding of phenoprodifen shifts the equilibrium between the inactive and active states of the H_1R toward the active state. The highly conserved $Trp^{6.48}$ is involved in a rotamer toggle switch during the process of receptor activation and shows a vertical orientation with respect to lipid bilayer in the inactive state (Fig. 4A), but a parallel orientation in the active state (Fig. 4B) of a GPCR (Crocker et al., 2006). For orientation 1 of **13** (Fig. 4A), the MD simulations showed a nearly vertical orientation of $Trp^{6.48}$, reflecting the inactive state at hH_1R as well as at gpH_1R. In contrast, for orientation 2 (Fig. 4B) of **13**, the MD simulation revealed a planar orientation of $Trp^{6.48}$ as proposed for the active state of a GPCR. Based on these results, it is suggested that phenoprodifens stabilize the inactive state in orientation 1 but the active state of H_1R in orientation 2. Because orientation 1 is the preferred one at hH_1R, whereas orientations 1 and 2 are established in comparable fractions at gpH_1R, the reduced efficacy of **13** at hH_1R compared with gpH_1R can be explained.

Pharmacology of Small Chiral Phenylhistamines and Chiral Phenoprodifens. For the small phenylhistamines **3R** and **3S**, the *S*-enantiomer showed a significantly higher affinity and potency than the *R*-enantiomer at all four species isoforms. The introduction of the additional methyl group in **3R** and **3S** compared with phenylhistamine **2** led to a significant decrease in efficacy. However, the picture is different for the chiral phenoprodifens **14R** and **14S**. In this case, only at hH_1R does the *S*-enantiomer possess the higher affinity; at bH_1R, rH_1R, and gpH_1R, the *R*-enantiomer possesses higher affinity. As already mentioned, molecular dynamics simulations showed that the chiral phenoprodifens can bind in two different orientations in analogy to the two orientations of the unsubstituted phenoprodifen. Based on these experimental results, concerning affinity, it is suggested that at hH_1R, the amount of orientation 2 of the chiral phenoprodifens is increased compared with the unsubstituted phenoprodifen **13**. Besides that, the additional methyl group, proposed to be located in the same pockets as the analog methyl groups for **3R** and **3S**, led to a decrease in efficacy for **14R** and **14S**.

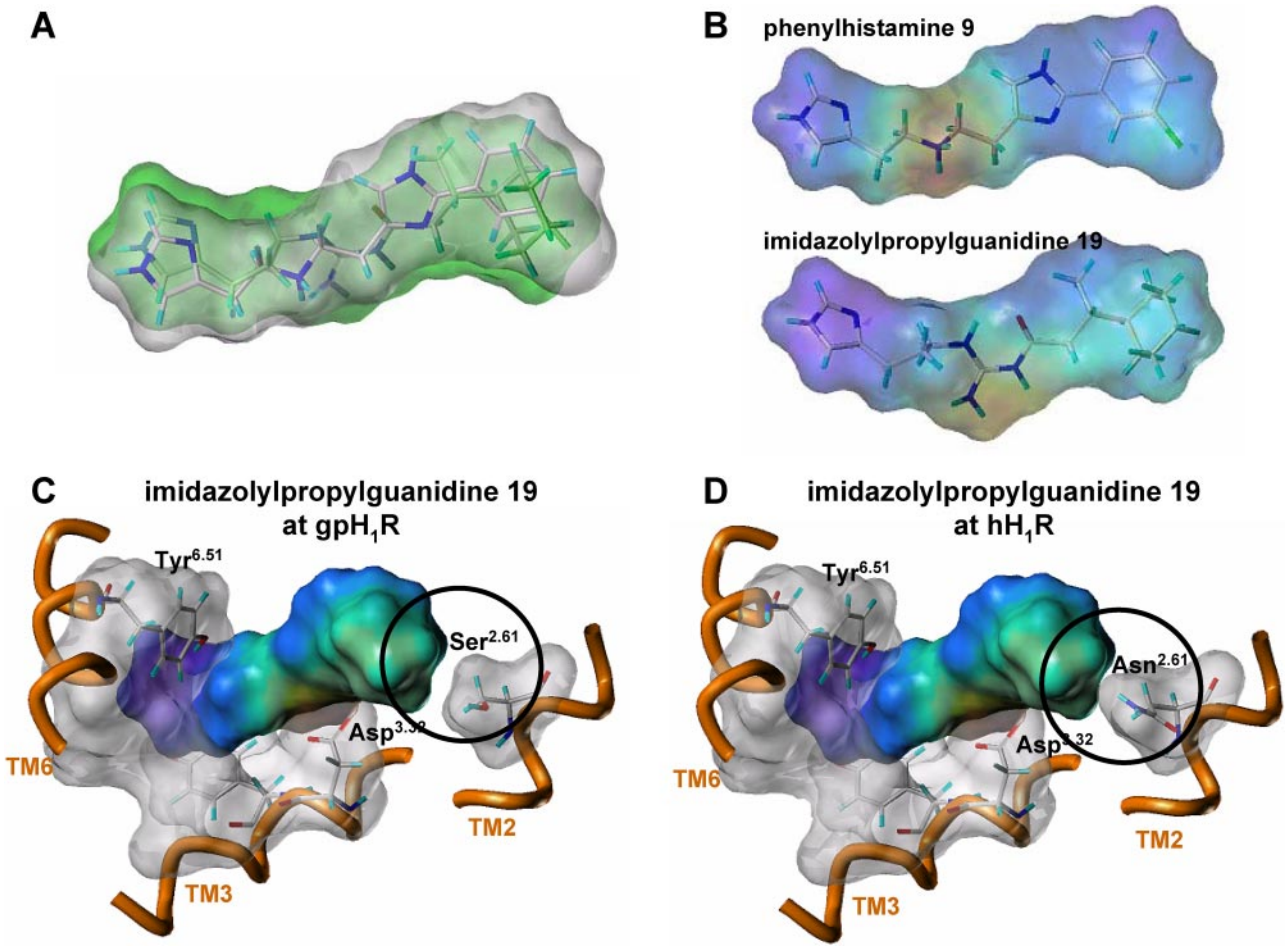

Fig. 7. Comparison of phenylhistamine **9** and imidazolylpropylguanidine **19** in the binding pocket of gpH_1R and hH_1R. A, multifit alignment of phenylhistamine **9** (gray shading) and imidazolylpropylguanidine **19** (green shading). B, the electrostatic potential surface of phenylhistamine **9** and imidazolylpropylguanidine **19**. C, binding mode of **19** at gpH_1R received by MD simulations. D, binding mode of **19** at hH_1R, received by MD simulations. The multifit alignment, the calculation of electrostatic potential surface and MD-simulations were performed as described in *Materials and Methods*. B to D, for the ligand, the electrostatic potential surface is shown: red indicates positive charge, blue indicates negative charge. C and D, the van der Waals surfaces of the most important amino acid side chains that are interacting with the ligand are given in gray shading.

Pharmacology of Phenylhistamines 7, 8, and 9 and Imidazolylpropylguanidine 19 (UR-AK57) at hH_1R and hH_2R-$G_s\alpha_S$. A recent study (Xie et al., 2006) revealed that the imidazolylpropylguanidine **19** (UR-AK57; Fig. 1) acts as a partial agonist at hH_2R-$G_s\alpha_S$, hH_1R, and gpH_1R. The potency of **19** at hH_2R-$G_s\alpha_S$ is significantly higher than at hH_1R. In addition, the potency of **19** is decreased at gpH_1R (pEC_{50}, 6.12 ± 0.06) compared with hH_1R. Thus, **19** is the first synthetic agonist with higher potency at hH_1R than at gpH_1R. Our data show that phenylhistamines **8** and **9** possesses a significantly higher potency at hH_1R compared with gpH_1R, as is the case for **19**. Thus, there are now three synthetic agonists with a higher potency at hH_1R compared with gpH_1R. In addition, the phenylhistamines **8** and **9** act as partial agonists at hH_2R-$G_s\alpha_S$. Compound **19** shows higher potency at hH_2R-$G_s\alpha_S$ than at hH_1R (Xie et al., 2006). In contrast, phenylhistamines **8** and **9** show higher potency at hH_1R than at hH_2R-$G_s\alpha_S$. Thus, whereas **19** exhibits selectivity for hH_2R compared with hH_1R, the opposite is true for **8** and **9**.

A comparison of imidazolylpropylguanidine **19** and phenylhistamines **8** and **9** at the level of ligand structure (Fig. 1) reveals differences, because imidazolylpropylguanidines and phenylhistamines represent different chemical classes, but also similarities. In particular, **19** as well as **8** and **9** possess free terminal imidazolyl moieties on the one hand, and an overlay of these ligands shows that they occupy similar volumes (Fig. 7A) with similar surface properties, like electrostatic potential (Fig. 7B). Most importantly, **19** possesses only one imidazole moiety. Thus, this compound can only bind in *one possible orientation* to the H_1R, with the histamine moiety in region between TM5 and TM3 and with the 3-cyclohexylbutanoyl moiety close to TM2 (Fig. 7, C and D), comparable with the binding modes 2 to 4 of **9** (Fig. 4, E and F). There is a gap between the cyclohexyl moiety of **19** and $Ser^{2.61}$ in gpH_1R (Fig. 7C) but a closer contact between the cyclohexyl moiety and $Asn^{2.61}$ in hH_1R. Accordingly, the van der Waals interaction between cyclohexyl moiety and $Asn^{2.61}$ is more effective than between cyclohexyl moiety and $Ser^{2.61}$, resulting in a higher potency at hH_1R compared with gpH_1R. Thus, it must be concluded that phenylhistamines **8** and **9** bind in modes 2–4, with the phenyl moiety located near TM2 of the H_1R. However, because binding mode 4 is the most stable in MD simulations, binding mode 4 should be the preferred one.

Conclusions

Our studies reveal substantial pharmacological differences among human, bovine, rat, and guinea pig H_1R species isoforms for different classes of agonists, such as phenylhistamines and phenoprodifens. Our studies also show that bH_1R and rH_1R can be classified as intermediate between hH_1R and gpH_1R, but hH_1R is more similar to bH_1R and rH_1R is more similar to gpH_1R. In the present study, we have identified the first phenylhistamines possessing a higher affinity and potency at hH_1R than at gpH_1R. Thus, we further corroborate the concept that it is possible to obtain selective H_1R agonists with higher affinity for hH_1R than for gpH_1R. The advantage of the compounds studied herein compared with imidazolylpropylguanidines is that they possess higher selectivity relative to H_2R.

Acknowledgments

We thank A. Seefeld for performing the GTPase assays, J. Felixberger for performing some binding assays, and G. Wilberg for her competent help with the cell culture.

References

Ballesteros JA, Shi L, and Javitch JA (2001) Structural mimicry in G protein-coupled receptors: implications of the high-resolution structure of rhodopsin for structure-function analysis of rhodopsin-like receptors. *Mol Pharmacol* **60:**1–19.

Bruysters M, Jongejan A, Gillard M, van de Manakker F, Bakker RA, Chatelain P, and Leurs R (2005) Pharmacological differences between human and guinea pig histamine H_1 receptors: Asn^{84} (2.61) as key residue within an additional binding pocket in the H_1 receptor. *Mol Pharmacol* **67:**1045–1052.

Cheng Y and Prusoff WH (1973) Relationship between the inhibition constant (K_i) and the concentration of inhibitor which causes 50 per cent inhibition (I_{50}) of an enzymatic reaction. *Biochem Pharmacol* **22:**3099–3108.

Cherezov V, Rosenbaum DM, Hanson MA, Rasmussen SG, Thian FS, Kobilka TS, Choi HJ, Kuhn P, Weis WI, Kobilka BK, et al. (2007) High-resolution crystal structure of an engineered human β_2-adrenergic G protein-coupled receptor. *Science* **318:**1258–1265.

Crocker E, Eilers M, Ahuja S, Hornak V, Hirshfeld A, Sheves M, and Smith SO (2006) Location of Trp2.65 in metarhodopsin II: implications for the activation mechanism of the visual receptor rhodopsin. *J Mol Biol* **357:**163–172.

Elz S, Kramer K, Pertz HH, Detert H, ter Laak AM, Kühne R, and Schunack W (2000) Histaprodifens: synthesis, pharmacological in vitro evaluation, and molecular modeling of a new class of highly active and selective histamine H_1-receptor agonists. *J Med Chem* **43:**1071–1084.

Gantz I, Munzert G, Tashiro T, Schäffer M, Wang L, DelValle J, and Yamada T (1991) Molecular cloning of the human histamine H_2 receptor. *Biochem Biophys Res Commun* **178:**1386–1392.

Hill SJ, Ganellin CR, Timmerman H, Schwartz JC, Shankley NP, Young JM, Schunack W, Levi R, and Haas HL (1997) International Union of Pharmacology. XIII. Classification of histamine receptors. *Pharmacol Rev* **49:**253–278.

Jongejan A, Bruysters M, Ballesteros JA, Haaksma E, Bakker RA, Pardo L, and Leurs R (2005) Linking agonist binding to histamine H_1 receptor activation. *Nat Chem Biol* **1:**98–103.

Kelley MT, Bürckstümmer T, Wenzel-Seifert K, Dove S, Buschauer A, and Seifert R (2001) Distinct interaction of human and guinea pig histamine H_2-receptor with guanidine-type agonists. *Mol Pharmacol* **60:**1210–1225.

Kunze M (2006) Histamin-H_1-Rezeptoragonisten vom Suprahistaprodifen- und 2-Phenylhistamin-Typ und 2-substituierte Imidazolylpropan-Derivate als Liganden für $H_1/H_2/H_3/H_4$-Rezeptoren—Neue Synthesestrategien und pharmakologische Testung. Ph.D. dissertation, University of Regensburg, Regensburg, Germany.

Leschke C, Elz S, Garbarg M, and Schunack W (1995) Synthesis and histamine H_1 receptor agonist activity of a series of 2-phenylhistamines, 2-heteroarylhistamines, and analogues. *J Med Chem* **38:**1287–1294.

Ligneau X, Morisset S, Tardivel-Lacombe J, Gbahou F, Ganellin CR, Stark H, Schunack W, Schwartz JC, and Arrang JM (2000) Distinct pharmacology of rat and human histamine H_3 receptors: role of two amino acids in the third transmembrane domain. *Br J Pharmacol* **131:**1247–1250.

Lovenberg TW, Roland BL, Wilson SJ, Jiang X, Pyati J, Huvar A, Jackson MR, and Erlander MG (1999) Cloning and functional expression of the human histamine H_3 receptor. *Mol Pharmacol* **55:**1101–1107.

Menghin S, Pertz HH, Kramer K, Seifert R, Schunack W, and Elz S (2003) N^{α}-imidazolylalkyl and pyridylalkyl derivatives of histaprodifen: synthesis and in vitro evaluation of highly potent histamine H_1-receptor agonists. *J Med Chem* **46:**5458–5470.

Moguilevsky N, Varsalona F, Noyer M, Gillard M, Guillaume JP, Garcia L, Szpirer C, Szpirer J, and Bollen A (1994) Stable expression of human H_1-histamine-receptor cDNA in Chinese hamster ovary cells. Pharmacological characterisation of the protein, tissue distribution of messenger RNA and chromosomal localisation of the gene. *Eur J Biochem* **224:**489–495.

Niv MY, Skrabanek L, Filizola M, and Weinstein H (2006) Modeling activated states of GPCRs: the rhodopsin template. *J Comput Aided Mol Des* **20:**437–448.

Oda T, Morikawa N, Saito Y, Masuho Y, and Matsumoto S (2000) Molecular cloning and characterization of a novel type of histamine receptor preferentially expressed in leukocytes. *J Biol Chem* **275:**36781–36786.

Oostenbrink C, Villa A, Mark AE, and van Gunsteren WF (2004) A biomolecular force field based on the free enthalpy of hydration and solvation: The GROMOS force-field parameter sets 53A5 and 53A6. *J Comput Chem* **25:**1656–1676.

Pertz HH, Görnemann T, Schurad B, Seifert R, and Strasser A (2006) Striking differences of action of lisuride stereoisomers at histamine H_1 receptors. *Naunyn Schmiedebergs Arch Pharmacol* **374:**215–222.

Preuss H, Ghorai P, Kraus A, Dove S, Buschauer A, and Seifert R (2007a) Mutations of Cys-17 and Ala-271 in the human histamine H_2 receptor determine the species selectivity of guanidine-type agonists and increase constitutive activity. *J Pharmacol Exp Ther* **321:**975–982.

Preuss H, Ghorai P, Kraus A, Dove S, Buschauer A, and Seifert R (2007b) Point mutations in the second extracellular loop of the histamine H_2 receptor do not affect the species-selective activity of guanidine-type agonists. *Naunyn Schmiedebergs Arch Pharmacol* **376:**253–264.

Rasmussen SG, Choi HJ, Rosenbaum DM, Kobilka TS, Thian FS, Edwards PC, Burghammer M, Ratnala VR, Sanishvili R, Fischetti RF, et al. (2007) Crystal structure of the human β_2 adrenergic G-protein-coupled receptor. *Nature* **450:**383–387.

Rosenbaum DM, Cherezov V, Hanson MA, Rasmussen SG, Thian FS, Kobilka TS, Choi HJ, Yao XJ, Weis WI, Stevens RC, et al. (2007) GPCR engineering yields

high-resolution structural insights into β_2-adrenergic receptor function. *Science* **318:**1266–1273.
Seifert R, Wenzel-Seifert K, Burckstummer T, Pertz HH, Schunack W, Dove S, Buschauer A, and Elz S (2003) Multiple differences in agonist and antagonist pharmacology between human and guinea pig histamine H_1-receptor. *J Pharmacol Exp Ther* **305:**1104–1115.
Strasser A and Wittmann HJ (2007) Analysis of the activation mechanism of the guinea-pig histamine H_1-receptor. *J Comput Aided Mol Des* **21:**499–509.
Straßer A, Striegl B, Wittmann HJ, and Seifert R (2008a) Pharmacological profile of histaprodifens at four recombinant histamine H_1 receptor species isoforms. *J Pharmacol Exp Ther* **324:**60–71.
Straßer A, Wittmann HJ, and Seifert R (2008b) Influence of the N-terminus and E2-loop of the H_1R to species differences between human and guinea-pig histamine H_1 receptor. *J Pharmacol Exp Ther* **326:**783–791.
Thurmond RL, Desai PJ, Dunford PJ, Fung-Leung WP, Hofstra CL, Jiang W, Nguyen S, Riley JP, Sun S, Williams KN, et al. (2004) A potent and selective histamine H_4 receptor antagonist with anti-inflammatory properties. *J Pharmacol Exp Ther* **309:**404–413.
Xie SX, Kraus A, Ghorai P, Ye QZ, Elz S, Buschauer A, and Seifert R (2006) N^1-(3-Cyclohexylbutanoyl)-N^2-[3-(1*H*-imidazol-4-yl)propyl]guanidine (UR-AK57), a potent partial agonist for the human histamine H_1- and H_2-receptors. *J Pharmacol Exp Ther* **317:**1262–1268.
Zingel V, Leschke C, and Schunack W (1995) Developments in histamine H_1-receptor agonists. *Prog Drug Res* **44:**49–85.

Address correspondence to: Dr. Andrea Straßer, Department of Pharmaceutical and Medicinal Chemistry I, University of Regensburg, Universitätsstraße 31, D-93053 Regensburg, Germany. E-mail: andrea.strasser@chemie.uni-regensburg.de